Antimatter and Gravity (WAG 2013)
International Journal of Modern Physics: Conference Series
Vol. 30 (2014) 1460262 (9 pages)
© The Authors
DOI: 10.1142/S2010194514602622

World Scientific
www.worldscientific.com

Measuring $\bar{g}$ with AE$\bar{g}$IS, progress and perspectives

D. Krasnický[a,*], S. Aghion[b,c], O. Ahlén[d], C. Amsler[e], A. Ariga[e], T. Ariga[e], A. S. Belov[f], K. Berggren[d], G. Bonomi[g,h], P. Bräunig[i], J. Bremer[d], R. S. Brusa[j], L. Cabaret[k], C. Canali[l], R. Caravita[b,m], F. Castelli[c,n], G. Cerchiari[o], S. Cialdi[c,n], D. Comparat[k], G. Consolati[c,p], H. Derking[d], S. Di Domizio[a,m], L. Di Noto[j], M. Doser[d], A. Dudarev[d], A. Ereditato[e], R. Ferragut[b,c], A. Fontana[h], P. Genova[h], M. Giammarchi[c], A. Gligorova[q], S. N. Gninenko[f], S. Haider[d], T. Huse[r], E. Jordan[o], L. V. Jørgensen[d], T. Kaltenbacher[d], J. Kawada[e], A. Kellerbauer[o], M. Kimura[e], A. Knecht[d], V. Lagomarsino[a,m], S. Lehner[s], A. Magnani[h,t], C. Malbrunot[d,s], S. Mariazzi[s], V. A. Matveev[f,u], G. Nebbia[v], P. Nédélec[w], M. K. Oberthaler[i], N. Pacifico[q], V. Petráček[x], C. Pistillo[e], F. Prelz[c], M. Prevedelli[y], C. Regenfus[l], C. Riccardi[h,t], O. Røhne[r], A. Rotondi[h,t], H. Sandaker[q], P. Scampoli[e,z], J. Storey[e], M. A. Subieta Vasquez[g,h], M. Špaček[x], G. Testera[a], E. Widmann[s], P. Yzombard[k], S. Zavatarelli[a] and J. Zmeskal[s]

[a] *Istituto Nazionale di Fisica Nucleare, Sez. di Genova, Via Dodecaneso 33, 16146 Genova, Italy*
[b] *Politecnico di Milano, LNESS and Dept of Physics, Via Anzani 42, 22100 Como, Italy*
[c] *Istituto Nazionale di Fisica Nucleare, Sez. di Milano, Via Celoria 16, 20133 Milano, Italy*
[d] *European Organisation for Nuclear Research, Physics Department, 1211 Genève 23, Switzerland*
[e] *Albert Einstein Center for Fundamental Physics, Laboratory for High Energy Physics, University of Bern, 3012 Bern, Switzerland*
[f] *Institute for Nuclear Research of the Russian Academy of Sciences, Moscow 117312, Russia*
[g] *University of Brescia, Dept of Mech. and Indust. Engineering, Via Branze 38, 25133 Brescia, Italy*
[h] *Istituto Nazionale di Fisica Nucleare, Sez. di Pavia, Via Agostino Bassi 6, 27100 Pavia, Italy*
[i] *University of Heidelberg, Kirchhoff Institute for Physics, Im Neuenheimer Feld 227, 69120 Heidelberg, Germany*
[j] *Department of Physics, University of Trento and TIFPA-INFN, Via Sommarive 14, 38050 Povo, Trento, Italy*
[k] *Laboratoire Aimé Cotton, CNRS, Université Paris Sud, ENS Cachan, Bâtiment 505 Campus d'Orsay, 91405 Orsay Cedex, France*
[l] *University of Zurich, Physics Institute, Winterthurerstrasse 190, 8057 Zürich, Switzerland*
[m] *University of Genoa, Dept of Physics, Via Dodecaneso 33, 16146 Genova, Italy*
[n] *University of Milano, Dept of Physics, Via Celoria 16, 20133 Milano, Italy*
[o] *Max Planck Institute for Nuclear Physics, Saupfercheckweg 1, 69117 Heidelberg, Germany*
[p] *Politecnico di Milano, Dept of Aerospace Sci. and Tech., Via La Masa 34, 20156 Milano, Italy*
[q] *University of Bergen, Institute of Physics and Technology, Alleegaten 55, 5007 Bergen, Norway*
[r] *University of Oslo, Dept of Physics, Sem Sælands vei 24, 0371 Oslo, Norway*
[s] *Stefan Meyer Institute for Subatomic Physics, Austrian Academy of Sciences, Boltzmanngasse 3, 1090 Vienna, Austria*
[t] *University of Pavia, Dept of Nuclear and Theoretical Physics, Via Bassi 6, 27100 Pavia, Italy*
[u] *Joint Institute for Nuclear Research, 141980 Dubna, Russia*
[v] *Istituto Nazionale di Fisica Nucleare, Sez. di Padova, Via Marzolo 8, 35131 Padova, Italy*
[w] *Claude Bernard University Lyon 1, Institut de Physique Nucléaire de Lyon, 4 Rue Enrico Fermi, 69622 Villeurbanne, France*
[x] *Czech Technical University in Prague, FNSPE, Břehová 7, 11519 Praha 1, Czech Republic*
[y] *University of Bologna, Dept of Physics, Via Irnerio 46, 40126 Bologna, Italy*
[z] *University of Napoli Federico II, Dept of Physics, Via Cinthia, 80126 Napoli, Italy*

[*] Presented by D. Krasnicky, daniel.krasnicky@ge.infn.it.

Received 14 January 2014
Revised 2 February 2014
Published 7 May 2014

AEḡIS experiment's main goal is to measure the local gravitational acceleration of antihydrogen $\bar{g}$ and thus perform a direct test of the weak equivalence principle with antimatter. In the first phase of the experiment the aim is to measure $\bar{g}$ with 1% relative precision. This paper presents the antihydrogen production method and a description of some components of the experiment, which are necessary for the gravity measurement. Current status of the AEḡIS experimental apparatus is presented and recent commissioning results with antiprotons are outlined. In conclusion we discuss the short-term goals of the AEḡIS collaboration that will pave the way for the first gravity measurement in the near future.

Keywords: Antimatter; gravity; antihydrogen; positronium; AEḡIS.

PACS Numbers: 04.80.−y, 07.77.Gx, 36.10.−k, 36.10.Dr, 36.10.Gv

1. Introduction

The main scientific goal of AEḡIS (Antimatter Experiment: Gravity, Interferometry and Spectroscopy)[1,2] is to measure the fall of antihydrogen ($\bar{\mathrm{H}}$) in the gravitational field of the Earth. Such measurement is a direct test of Einstein's Weak Equivalence Principle (WEP), which states that a trajectory of a falling test body depends only on its initial position and velocity, and is independent of its composition or structure. Although very precise measurements have been performed to test the WEP with ordinary matter,[3] there was no measurement done so far to test the gravitational interaction between matter and antimatter with even modest precision. Gravitational experiments were performed to study the fall of charged antimatter,[4,5] but were overwhelmed by systematic errors due to the strength of electromagnetic forces on a bare charge.[6] Recently, the ALPHA collaboration presented rough bounds on the gravitational acceleration of antihydrogen[7] by studying the $\bar{\mathrm{H}}$ annihilation position and the time of the release of antihydrogen atoms from a multi-polar magnetic trap. Within a 95% confidence interval the ratio $\bar{g}/g$ is in the range $-65 < \bar{g}/g < 110$.

AEḡIS collaboration plans to use a multitude of experimental techniques in order to measure the gravitational acceleration of antimatter $\bar{g}$ to, at first, 1% relative precision without theoretical assumptions.[a] The AEḡIS experimental apparatus is located at CERN laboratory in the Antiproton Decelerator (AD) hall. The gravity measurement in AEḡIS will be performed by producing a pulsed cold antihydrogen beam and observing its vertical deflection in a set of moiré deflectometer gratings.[8]

2. $\bar{\mathrm{H}}$ Production, Beam Formation and Gravity Measurement

Figure 1 shows schematically the AEḡIS antihydrogen production scheme. Antihydrogen will be produced using the charge exchange reaction between highly excited

---

[a] The chosen method is not limited to 1% precision and can be improved in future if transversal $\bar{\mathrm{H}}$ beam laser cooling schemes were implemented.

(Rydberg) positronium atom (Ps^*) and an antiproton $\bar{\mathrm{p}}$:

$$\mathrm{Ps}^* + \bar{\mathrm{p}} \rightarrow \bar{\mathrm{H}}^* + \mathrm{e}^- \tag{1}$$

Reaction (1) has many advantages, in particular: the reaction cross section scales as $\sigma \propto n_{\mathrm{Ps}}^4$, where n_{Ps} is the positronium principal quantum number and $\sigma \simeq 10^{-9}$ cm^2 for $n_{\mathrm{Ps}} \approx 20$. Another important advantage is that the quantum states of $\bar{\mathrm{H}}$ are determined by n_{Ps}, while the resulting antihydrogen temperature is given by the temperature of antiprotons prior to formation. Charge exchange reaction is thus well suited for production of low temperature antihydrogen in a controlled state.

In order to make use of the very large cross sections offered by reaction (1) AE$\bar{\mathrm{g}}$IS will produce and subsequently excite positronium to Rydberg states. Positronium will then fly into a Penning trap with trapped and cold 0.1 K antiproton cloud, where reaction (1) will take place.

The newly formed $\bar{\mathrm{H}}$ will not remain confined in the Penning trap and will slowly spread out isotropically with its thermal velocity distribution ($v \approx 25 - 80$ m/s). At this point we will use another feature of the charge exchange reaction, namely the fact that $\bar{\mathrm{H}}$ is produced in Rydberg states. Such states have large electric dipole moment and are sensitive to inhomogeneous electric fields. Using an electric field gradient AE$\bar{\mathrm{g}}$IS will accelerate the high (or low) field-seeking $\bar{\mathrm{H}}$ and form a beam with 0.1 K thermal transversal velocity distribution, and with a longitudinal velocity up to ≈600 m/s. Details on the beam formation in AE$\bar{\mathrm{g}}$IS can be found in Ref. 9.

2.1. *Positronium production and excitation*

As can be seen in Fig. 1 the positronium necessary for the antihydrogen production will be produced in a positron-positronium conversion target. Positrons will be accelerated up to an energy of 7 keV and implanted into a nanoporous silica target. In such target material, where the pores are composed of ordered nano-channels,

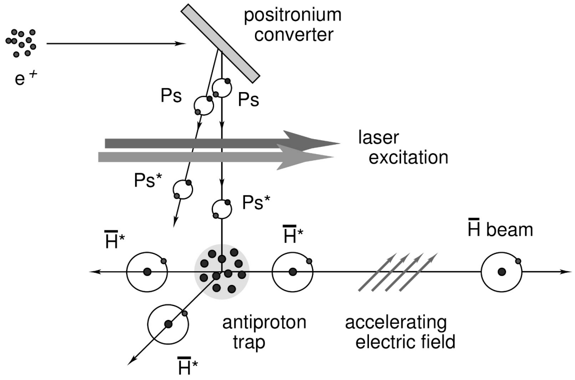

Fig. 1. Schematic of pulsed antihydrogen production in AE$\bar{\mathrm{g}}$IS.[2]

a large fraction of orto-positronium is emitted into vacuum.[10] As the positronium exits the pores it will be excited to Rydberg levels by two superimposed laser pulses. The laser system (currently fully functional) consists of a UV pulse (205 nm) that induces the $n_{\mathrm{Ps}}=1 \rightarrow 3$ transition and a tunable IR laser pulse (1650-1700 nm), which allows for subsequent excitation to $n_{\mathrm{Ps}}=16$–30 levels.[11]

2.2. *Gravity measurement*

The gravitational acceleration $\bar{g}$ of antihydrogen will be measured by studying the deflection due to gravity of the $\bar{\mathrm{H}}$ beam as it flies through a moiré deflectometer.[8] The deflectometer is a classical device composed of two horizontal gratings and a third equidistant plane, where a shadow-like fringe pattern is created. The vertical position of the fringes depends on the atom beam velocity and on the force acting on the beam. In the case of AE$\bar{\mathrm{g}}$IS the third plane will be a hybrid position sensitive detector with a high spatial resolution. The deflectometer gratings will have 40 μm pitch and 30% open fraction. If L is the length between the gratings (and the detector) and v is the velocity of the beam, then the vertical shift due to gravity δx in the deflectometer is:

$$\delta x = -g\frac{L^2}{v^2}\ . \tag{2}$$

In AE$\bar{\mathrm{g}}$IS the flux of antihydrogen will be rather low, it is expected to produce between ten to a few 100 $\bar{\mathrm{H}}$ atoms every 300 s (three $\bar{\mathrm{p}}$ shots from the AD). The advantage of a such low flux is that the time of individual $\bar{\mathrm{H}}$ hits on the detector will be measured and thus the beam does not have to be monochromatic. To determine $\bar{g}$ using Eq. (2) we will measure the time-of-flight of each $\bar{\mathrm{H}}$ that annihilates on the detector and its vertical position (δx).

The position sensitive detector will be composed of a silicon micro-strip detector and followed by a replaceable nuclear emulsion detector and a fiber tracker.[12, 13] The main advantage of the moiré deflectometer is that neither a collimated nor ultracold nor monochromatic beam is necessary to perform a measurement with required precision. Schematic of the so-called gravity measurement module, which includes the gratings and the position sensitive detectors can be seen in Fig. 2.

The overall design of the detector is challenging not only for the requested to the high resolution (2-8 μm), but also because it has to work in cryogenic conditions.[b] The nuclear emulsion detector offers an unmatched spatial resolution of few microns and thus increases significantly the sensitivity of the deflectometer, but it cannot provide time information. The silicon micro-strip detector, on the other hand, combines very good resolution (≈ 8 μm) with the time information, that the emulsion needs. The scintillating fiber tracker at the back of the emulsion improves the overall

---

[b] Currently R&D within the collaboration is underway in order to determine at which cryogenic temperature the system is feasible (either 4 or 77 K).

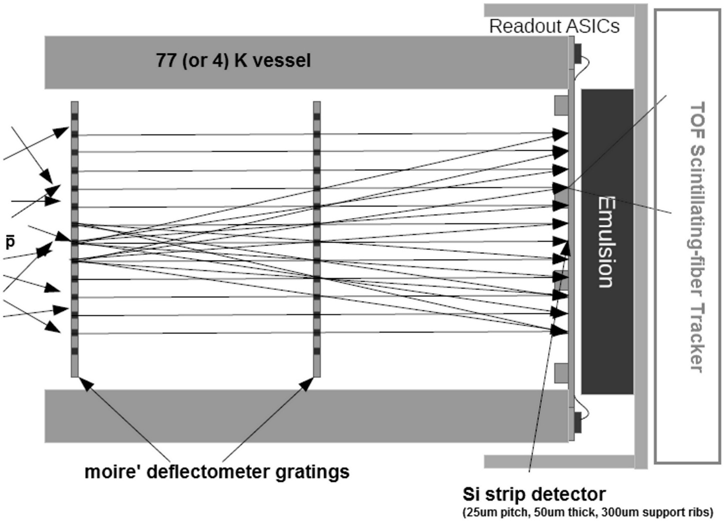

Fig. 2. Schematic of the "gravity module" of AEḡIS (currently in development). The moiré deflectometer gratings and 50 μm thick Si detector (all equidistant) are located inside a UHV cryogenic chamber. The Si strip detector acts as an active vacuum window, right behind it in the high vacuum region and at cryogenic temperature is the nuclear emulsion detector, followed by a scintillating fiber tracker.

detection efficiency and provides a "rough" x-y information[c] of each $\bar{\mathrm{H}}$ annihilation so that the precise position can be extracted from the emulsion and associated with a correct time-of-flight information. If neglecting the systematic errors only 1000 reconstructed $\bar{\mathrm{H}}$ atoms are necessary for a 1% $\bar{g}$ measurement,[12] which is an order of magnitude improvement with respect to the original AEḡIS proposal.[1]

3. Status of the AEḡIS Experimental Apparatus

AEḡIS caught the first antiprotons from the Antiproton Decelerator (AD) in 2012. During 2013 there were no antiprotons available at CERN and thus commissioning of the system with positrons and electrons took place. An overall view of the experiment is shown in Fig. 3. The positrons (see Sec. 3.1) are transferred through the positron transfer line into the main AEḡIS cryogenic traps located inside the 5 T and 1 T superconducting magnets. The antiprotons from the decelerator are slowed down in a set of degrading foils and subsequently caught in traps located in the high (5 T) magnetic field (Sec. 3.2), where they are also cooled to eV energies. They are then transferred into the 1 T trap system (Sec. 3.3), where the final cooling and $\bar{\mathrm{H}}$ production and beam formation take place.

---

[c] A precise value has not yet been set, but the resolution will be in the order of 250μm.

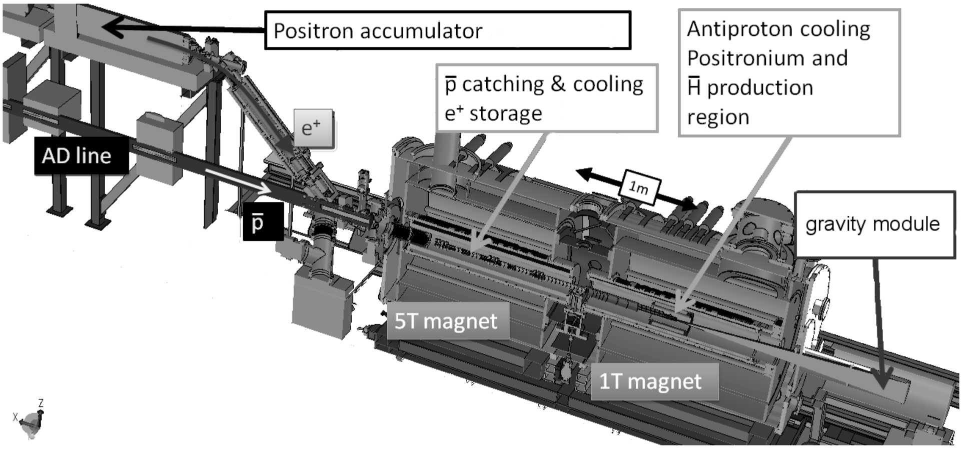

Fig. 3. A cut-open view of AEḡIS experimental apparatus. The gravity module is only schematically drawn and is currently in design and development phase.

3.1. *Positron accumulator system*

The positron accumulator[14] system of AEḡIS is composed of a ^{22}Na β^+ source, a solid neon moderator, a CO_2 buffer gas trap and an accumulator. The system, along with a positron transfer line (see Fig. 3), is now complete. Once a sufficient number of e^+ is accumulated they are transported into the 5 T and subsequently 1 T magnet where the Ps production will take place. To produce sufficient amount of Ps for $\bar{H}$ produciton, large quantities of positrons are necessary. Currently, in 330 s 3×10^7 e^+ have been stored using a 740 MBq source. It is expected to reach the nominal design value of 10^8 e^+ within this year. In addition, after the commissioning phase is completed, an order of three times stronger radioactive source is foreseen to boost the number of available positrons in the future.

A new vacuum chamber designed for studies of positronium has been installed in late 2013 at the output of the positron accumulator. This chamber has a built-in e^+ buncher and allows to measure Ps conversion efficiency of various target materials at cryogenic temperatures and study the ideal parameters of laser excitation. The chamber is being commissioned and first measurements will take place soon.

3.2. $\bar{p}$ *catching traps*

In 2012, the Penning-Malmberg trap built for catching and cooling of $\bar{p}$ and e^+ in AEḡIS has been tested for the first time.[15] The trap is built in a multi-ring geometry with electrode radii of 15 mm and it is located in a cold bore (7 K) of the 5 T superconducting magnet. Along the 1 m long stack of electrodes three high voltage catching electrodes are inserted. In this way two $\bar{p}$ catching lengths of 46 cm or 76 cm are available. Approximately 1.3×10^5 $\bar{p}$ per one AD shot are caught using a 9 kV voltage (nominal) on the catching electrodes. 90% of caught antiprotons are then cooled to eV-range within 40 s by a pre-loaded cloud of $\sim 10^9$ electrons located in a smaller 120 V deep potential well.

During the 2012 run with antiprotons[d] the lifetime of cold $\bar{p}$ was of the order of 600 s, which allowed to perform tests of stacking of multiple shots of antiprotons. The limiting lifetime was caused by the insufficient vacuum level, which was estimated to be approximately 8×10^{-13} mbar in the trap region. For this reason a modification of the vacuum system has been performed in 2013, which led to a factor two improvement in the room temperature vacuum level. In addition the temperature of the cryogenic system has been lowered and we expect that the lifetime of $\bar{p}$ will improve by a factor two to four in the future runs, which should be adequate for the catching and cooling needs in this trap system.

3.3. *1 T trap system*

The trap system located in the 1 T superconducting magnet is a complex system of cylindrical Penning-Malmberg traps. As can be seen in Fig. 4, the system comprises of four electrode regions with diverse requirements.

The first part is a large radius ($r = 22$ mm) trap, which serves as a preparation trap after the transfer of particles from the 5 T magnet. In this trap the particle clouds, which form a non-neutral plasma, are compressed with the rotating wall drive.[16] The large trap splits into two traps with 5 mm inner radii. The on-axis trap is dedicated for antiproton transfer towards the $\bar{H}$ production trap, which is a novel cylindrical multi-ring Penning trap design with a semi-transparent mesh (for positronium passage) and equipped with low noise electronics. This trap is where the cooling of antiprotons to final temperatures will take place. At the moment the trap temperature is 7 K. A dilution refrigerator that could bring the temperature down to 100 mK is under development by the collaboration.

Another function of the large radius trap is to move positron plasma off-axis into the positron high voltage trap, which is used to accelerate positrons onto the Ps conversion target. The movement of positrons off-axis is performed by the excitation

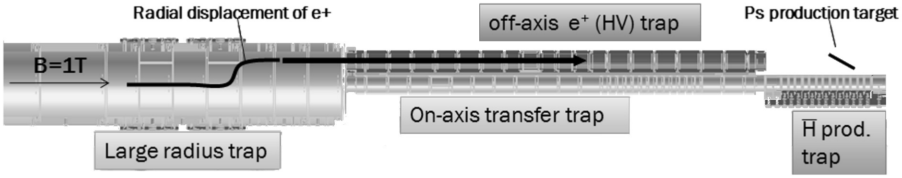

Fig. 4. Schematic of AE$\bar{g}$IS 1 T trap system. Excitation of the diocotron mode of e^+ plasma used to load positrons into the off-axis trap is schematically shown.

---

[d] The accelerator complex at CERN is under maintenance during 2013 and part of 2014 and so no more antiprotons were available up to now.

of the diocotron mode of e^+ plasma.[17] Currently the AE$\bar{\text{g}}$IS trap system is being commissioned with electrons and positrons.

3.4. *Detector tests*

During the 2012 antiproton run various detectors were tested with 100 keV antiprotons. Direct annihilations of $\bar{\text{p}}$ on silicon and nuclear emulsion detectors were measured. Besides testing the response of various detectors to direct annihilation, Monte-Carlo simulation tools (using GEANT 4) were confronted with low energy antiproton data (for the first time in case of silicon). These detector tests pave the way towards the development of the final position sensitive detector suitable for gravity measurement in AE$\bar{\text{g}}$IS . The results can be found in Refs. 12 and 13.

4. Conclusions

AE$\bar{\text{g}}$IS plans to measure for the first time the gravitational acceleration of antihydrogen $\bar{g}$ to (at first) 1% relative precision. Most parts of AE$\bar{\text{g}}$IS have been constructed and are currently being commissioned with electrons and positrons. Some important experimental techniques have already been successfully implemented: efficient $\bar{\text{p}}$ catching and pre-cooling to eV-range or positron accumulation, which is close to its foreseen performance. The work on the final design of the moiré deflectometer and on the hybrid position sensitive detector are underway and production of the gravity measurement module will start soon.

The short term plans of AE$\bar{\text{g}}$IS are to test all the remaining components and techniques necessary for $\bar{\text{H}}$ production. This includes the transfer of positrons, the positronium production and laser Ps excitation and also the transfer and the cooling of antiprotons. In parallel to the main experimental program we are preparing the positronium test chamber in order to perform measurements on the Ps conversion efficiency, Ps time-of-flight and Rydberg positronium spectroscopy.

References

1. M. Amoretti *et al.*, *Proposal for the AEGIS experiment at the CERN antiproton decelerator*, Tech. Rep. SPSC-P-334. CERN-SPSC-2007-017, CERN (Geneva, 2007).
2. M. Doser *et al.*, *Classical and Quantum Gravity* **29**, p. 184009 (2012).
3. E. Adelberger *et al.*, *Progress in Particle and Nuclear Physics* **62**, 102 (2009).
4. M. Holzscheiter *et al.*, *Nuclear Physics A* **558**, 709 (1993).
5. F. C. Witteborn and W. M. Fairbank, *Nature* **220**, 436 (1968).
6. T. W. Darling *et al.*, *Rev. Mod. Phys.* **64**, 237 (1992).
7. C. Amole *et al.*, *Nature Communications* **4**, 1785 (2013).
8. M. K. Oberthaler *et al.*, *Phys. Rev. A* **54**, 3165 (1996).
9. G. Testera *et al.*, *AIP Conference Proceedings* **1037**, 5 (2008).
10. S. Mariazzi *et al.*, *Phys. Rev. B* **81**, 235418 (2010).
11. S. Cialdi *et al.*, *Nucl. Instrum. Meth. B* **269**, 1527 (2011).
12. S. Aghion *et al.*, *Journal of Instrumentation* **8**, P08013 (2013).
13. S. Aghion *et al.*, **arXiv:1311.4982** (2013), Submitted to Journal of Instrumentation.

14. R. G. Greaves, M. D. Tinkle and C. M. Surko, *Physics of Plasmas* **1**, 1439 (1994).
15. D. Krasnický *et al.*, *AIP Conference Proceedings* **1521**, 144 (2013).
16. D. H. E. Dubin and T. M. O'Neil, *Rev. Mod. Phys.* **71**, 87 (1999).
17. C. Canali *et al.*, *European Physical Journal D* **65**, 499 (2011).